Asian Journal of Current Research in Clinical Cancer
ISSN: 3062-4444
2025, Volume 5, Issue 2, Page No: 12-21

Available online at: www.galaxypub.co/page/journals

Galaxy Publication

Heterogeneous High-Dose Testosterone Resistance in CRPC: Three Novel Cell Models Recapitulate Clinical Variability

S. Benali[1*], M. Khedidja[1], A. Tarek[1]

[1]Department of Cancer Biology, School of Medicine, University of Algiers, Algiers, Algeria.

***E-mail** ✉ algiers.bio.89@yahoo.com

Received: 19 April 2025; **Revised:** 01 August 2025; **Accepted:** 03 August 2025

ABSTRACT

Administering testosterone at levels exceeding the physiological range, especially when alternated with anti-androgen therapy in men with metastatic castration-resistant prostate cancer (CRPC), has yielded notable benefits in clinical trials. As this approach becomes increasingly implemented in practice, it is essential to clarify how resistance develops. For this purpose, three distinct CRPC cell models responsive to testosterone were independently generated. From each model, lines resistant to high-dose testosterone (HTR) were selected. The three parental CRPC lines exhibited different sensitivities to elevated testosterone exposure in both in vitro and in vivo systems. The derived HTR variants showed stable resistance to testosterone and diverse responses to its withdrawal in animal studies. The variability in hormonal reaction corresponded to differences in androgen receptor (AR) expression within each cell population. These results present three HTR models suitable for probing the mechanisms underlying resistance to supraphysiologic testosterone and for exploring new therapeutic strategies.

Keywords: Prostate cancer, Supraphysiologic testosterone, Cell culture models, Androgen resistance, Androgen deprivation

How to Cite This Article: Benali S, Khedidja M, Tarek A. Heterogeneous High-Dose Testosterone Resistance in CRPC: Three Novel Cell Models Recapitulate Clinical Variability. Asian J Curr Res Clin Cancer. 2025;5(2):12-21. https://doi.org/10.51847/xsdep8Rw88

Introduction

Even with major advances over the past decade in managing metastatic prostate cancer, it continues to rank as the second most common cause of cancer mortality among men in the United States [1, 2]. In the early stages, tumor growth depends heavily on androgen receptor–mediated signaling, and androgen deprivation therapy (ADT) remains the cornerstone for advanced cases [3]. Eventually, resistance to ADT arises, producing the aggressive form known as castration-resistant prostate cancer (CRPC). Despite the availability of several newer drugs, treatment options for CRPC remain limited [4-11].

Interestingly, a subset of CRPC patients benefits from very high doses of testosterone. One such method, bipolar androgen therapy (BAT), cycles serum testosterone between extremely high and near-castrate concentrations through monthly testosterone injections [12]. In the Phase II TRANSFORMER study, 28.2% of men whose cancer had progressed on abiraterone acetate experienced a ≥50% decline in PSA levels after BAT. Notably, BAT also appeared to restore sensitivity to androgen receptor–targeted treatment—77.8% of patients responded to enzalutamide following BAT [13]. Comparable results were observed in a smaller study involving men previously unresponsive to enzalutamide [14]. Nonetheless, progression during or after supraphysiologic testosterone therapy is common, underscoring the importance of uncovering resistance mechanisms in both testosterone-naïve and testosterone-resistant CRPC. A deeper understanding of these mechanisms could facilitate the design of combination therapies or identify biomarkers predictive of testosterone responsiveness.

A central difficulty in CRPC drug development is the pronounced heterogeneity between and within tumors. Therefore, laboratory models that reproduce this variability are crucial. We generated three CRPC cell models sensitive to high-dose testosterone, together with resistant counterparts, that mirror the diversity seen in patient

tumors. Their reactions to testosterone exposure and subsequent withdrawal were analyzed both in vitro and in vivo, demonstrating that differences in AR expression influence treatment outcomes. These models provide a robust platform for testing novel therapeutic interventions for high-dose testosterone–resistant CRPC.

Materials and Methods

Cell lines

All experimental lines originated from the LNCaP prostate cancer cell line, obtained from the University of Colorado Cancer Center (UCCC, Aurora, CO, USA) and validated through short tandem repeat profiling. The process of deriving LNCaP variants has been described earlier [15]. The P1 variant was established by repeated passaging under low-androgen conditions. The M1 and M2 lines were first cultured in media containing the androgen receptor blocker enzalutamide, followed by further selection in low-androgen media. From each of these three CRPC lines, high-dose testosterone–resistant (HTR) derivatives were produced through continued passage in low-androgen medium supplemented with 1 nM R1881 (synthetic androgen). The resistant lines were designated P1R1/R, M1R1/R, and M2R1/R.

Clonogenic assay

For the clonogenic analysis, 24-well plates were seeded with 2000 cells per well in media containing charcoal-stripped serum (CSS) and varying concentrations of the indicated compounds. Cultures were maintained for at least 14 days. Once any well-reached confluence, all wells on the plate were fixed and processed. Each plate contained a single cell line, and results were standardized to its own untreated control. All treatments were performed in four replicate wells. Colonies were stained using crystal violet, imaged, and quantified using ImageJ (https://imagej.net/ij; version 1.51j8, Java 1.8.0_112, 64-bit), with colony area determined using a validated plugin (https://journals.plos.org/plosone/article?id=10.1371/journal.pone.0092444; accessed 8 March 2022).

In vivo tumor implantation

Athymic nude male mice (sourced from Jackson and Envigo Laboratories, Bar Harbor, ME, USA) were maintained at the University of Colorado Animal Center and surgically castrated at 6–8 weeks of age. Under isoflurane/oxygen anesthesia, tumor cells (2,000,000 per injection) were introduced subcutaneously into both flanks in 100 µL of Matrigel using a 27–30 G needle. For CRPC line experiments, implantation was carried out one week post-castration, whereas for HTR lines, cells were injected one week following testosterone pellet insertion.

Testosterone pellet implantation

After providing extended-release buprenorphine for analgesia, a 12.5 mg sustained-release testosterone pellet (Innovative Research of America, Sarasota, FL, USA; NA-151) was placed beneath the skin roughly one week after surgical castration in experiments using HTR-derived models. This timing was chosen because early work with P1R1/R showed that tumors failed to establish effectively in mice retaining normal physiological testosterone. Immunocompromised animals naturally maintain suppressed testosterone levels [16]. For CRPC cell line experiments, the testosterone pellets were introduced only after tumors had formed and were palpable, measuring approximately 300–500 mm^3. Using a 10-gauge trocar, a small incision was made at the posterior region, and the pellet was inserted subcutaneously between the shoulders. The opening was sealed with Vetbond surgical adhesive. When animals survived longer than 90 days after pellet placement, a replacement pellet was added following removal of the previous one if possible. In certain instances, the earlier pellet could not be extracted due to encapsulation or tissue overgrowth as the material degraded.

Testosterone pellet removal

Prior to removal, animals were anesthetized with isoflurane vapor, and buprenorphine ER was administered for postoperative pain relief. A short incision was created at the upper back, directly over the implant location, and the pellet was gently excised. The wound was closed using a single surgical clip, which was removed after 7–10 days, once complete healing was observed.

Tumor volume measurement

Tumor sizes were monitored with wireless Bluetooth calipers, and data were recorded twice weekly. When growth occurred on both flanks, the reported tumor volume represented the combined total of the two sites.

Tissue collection and immunohistochemical analysis

To determine androgen receptor (AR) expression in the tested lines, formalin-fixed tissue samples were sectioned at 5 µm thickness and processed for immunohistochemistry. The antibodies and dilutions were as follows: AR primary antibody (Cell Marque, Rocklin, CA, USA; #200R-15) at 1:200; secondary reagent (EnvisionPlus Rabbit, Dako, Glostrup, Denmark; #K4003); Ki67 primary (Thermo Scientific, Waltham, MA, USA; #RM-9106-S1) at 1:400; and horse anti-rabbit secondary (Vector Labs, Burlingame, CA, USA; #MP-7401). Samples from 3–6 mice carrying tumors from either CRPC or HTR lines were submitted blindly to a specialist pathologist (F.F.) for scoring. Random tumor fields were selected, photographed, and printed, while stromal regions were excluded from analysis.

Staining intensity for AR was graded using an H-score, where the signal intensity (0 = absent, 1 = weak, 2 = moderate, 3 = strong) was multiplied by the percentage of cells at each intensity, giving totals between 0 and 300. In all, 28 slides were analyzed, averaging 5,363 cells per slide (range 4,707–7,080).

Statistical analysis

Colony growth data were expressed relative to mean baseline proliferation in the absence of synthetic androgen. Differences between treatments and baseline were examined using the Wilcoxon exact rank-sum test. Tumor growth was mainly summarized using descriptive measures categorized by treatment type and cell model. Overall survival, defined as the number of days from testosterone implantation (or control match), was analyzed with the Kaplan–Meier estimator. Intergroup differences were determined by the log-rank test or, when proportional hazard assumptions were not satisfied, a two-stage hazard rate comparison [17]. Median survival and 95% confidence intervals were calculated, though upper limits could not be established due to the small cohort size and computational limits.

H-scores were compared between testosterone-sensitive CRPC and HTR CRPC using the Wilcoxon exact test. To correct for clustering among slides from the same line, a mixed-effects regression model with random intercepts was applied. To examine cell intensity distributions between matched groups, chi-square analyses were performed. All computations were conducted in R version 4.3.1 (R Core Team, Vienna, Austria), and $p < 0.05$ was considered statistically significant.

Results and Discussion

In vitro modeling of resistance to high-dose testosterone

The three CRPC lines (M1, M2, and P1) were grown in low-androgen media and treated with R1881, a synthetic androgen, at different concentrations **(Figure 1)** [15]. Each line showed a trend toward reduced colony formation following R1881 exposure, though the effect did not reach statistical significance. The M1 line showed a mild, nonsignificant increase at the 0.03 nM dose, whereas higher doses produced decreases in growth, none of which were statistically meaningful.

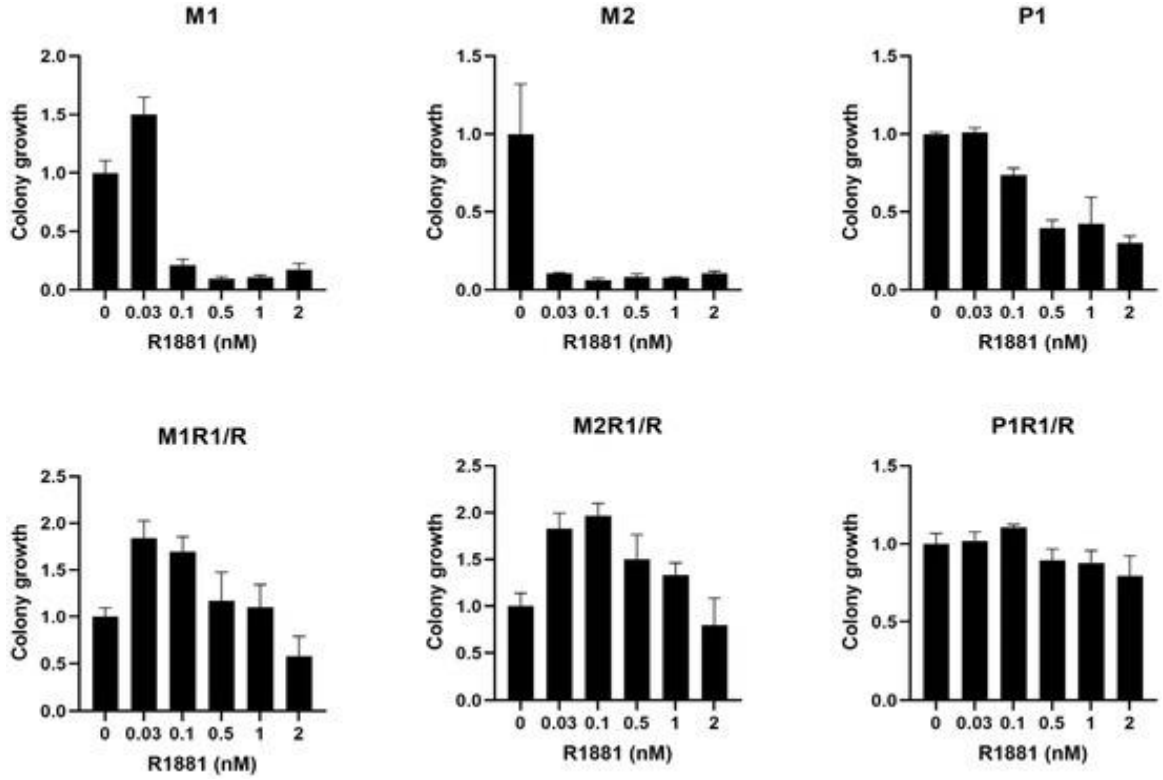

Figure 1. Clonogenic assay outcomes for CRPC and HTR cell lines exposed to synthetic androgen R1881.

Each HTR cell line was generated from its corresponding CRPC parent line through serial passage in a culture medium containing 1 nM R1881 and was designated M1R1/R, M2R1/R, and P1R1/R, respectively. As depicted in **Figure 1**, all three HTR lines exhibited similar proliferation rates under high-androgen conditions (1 nM R1881) compared with androgen-free medium. The hormone response pattern, however, differed among the variants: M1R1/R and M2R1/R displayed enhanced growth when exposed to lower androgen concentrations, while P1R1/R showed no appreciable change in growth across androgen levels up to 1 nM.

In vivo assessment of high-dose testosterone effects in CRPC models

To evaluate whether the in vitro–derived models accurately reflected CRPC and HTR prostate cancer behavior in vivo, tumor progression and overall survival were monitored in castrated male mice implanted with these cell lines and subjected to hormonal manipulation.

Each of the three CRPC-derived models (M1, M2, and P1) was injected into castrated hosts, with 10 (5 treated and 5 untreated), 17 (8 treated and 9 untreated), and 12 (6 treated and 6 untreated) mice analyzed per group, respectively.

After tumors became established and reached 300–500 mm^3, testosterone pellets were implanted. For each treated mouse, a tumor size–matched control without a pellet was maintained. Tumor measurements were taken before implantation and then twice weekly thereafter.

As shown in **Figure 2**, tumor volumes were compared at Day 30 following testosterone administration (or at euthanasia if tumor burden required earlier sacrifice). Responses to testosterone varied markedly across the three models. The P1 tumors grew rapidly under castration but were strongly suppressed by testosterone, occasionally regressing to barely palpable size. In contrast, M1 and M2 tumors exhibited slower growth and greater variability in their response to treatment.

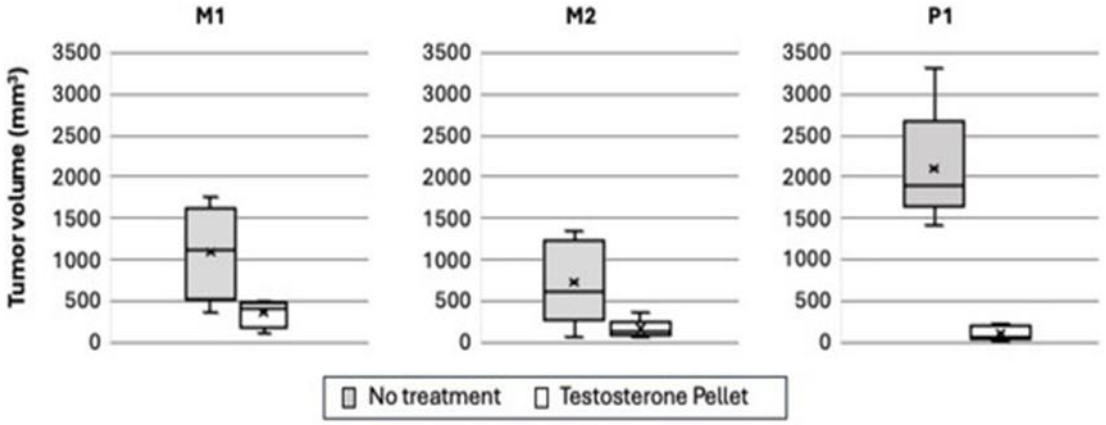

Figure 2. Tumor volume comparison of CRPC cell lines after testosterone implantation.

Tumor volumes, with and without testosterone pellets, are displayed at Day 30 or at the time of euthanasia if earlier due to excessive growth. The black central line represents the median (50th percentile); the box encloses the 25th–75th percentiles; whiskers show the 5th–95th percentiles; and x denotes the mean value.

The overall survival data for mice bearing these CRPC tumors are presented in **Figure 3**, measured as days since testosterone implantation or matched control date.

Mice receiving testosterone showed significant survival benefits in the M2 (Median: 95.5 days, 95% CI: 91–NA, $p = 0.03$) and P1 (Median: 104.5 days, 95% CI: 38–NA, $p = 0.01$) groups. The M1 line also demonstrated longer survival with testosterone (Median: 76 days, 95% CI: 37–NA), though this improvement did not reach significance ($p = 0.53$).

In M1 and M2, survival curves began to diverge around 50–60 days, whereas for P1, separation occurred earlier (20–30 days), likely reflecting its faster tumor kinetics and marked response to androgen exposure. Notably, two of six mice exhibited sustained survival approaching one year. One P1-treated mouse died from an unrelated cause, not associated with tumor size or experimental procedures.

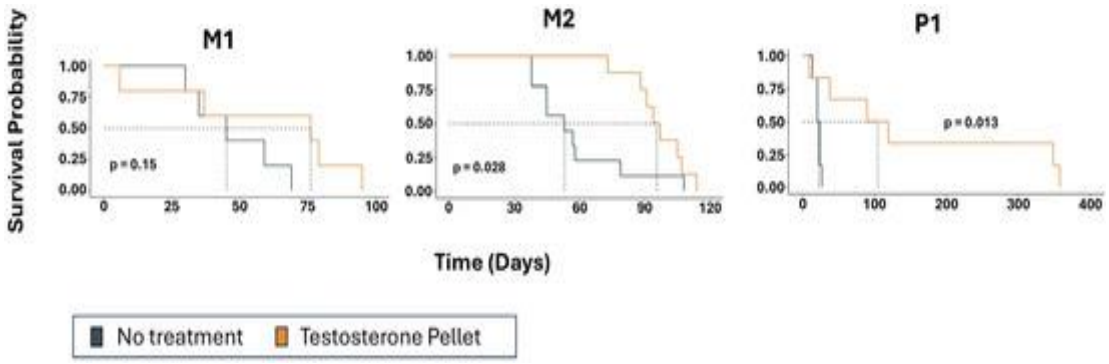

Figure 3. Survival outcomes for CRPC variants treated with testosterone or left untreated.

Depicted are survival curves for M1, M2, and P1 tumor-bearing mice, with testosterone-treated cohorts shown in orange and untreated controls in black. Note that the x-axis differs among variants. Day 0 represents the start of testosterone treatment or pairing for controls.

In vivo analysis of high-dose testosterone resistance

Next, the study explored whether in vitro–selected CRPC derivatives resistant to androgen exposure displayed an HTR phenotype in vivo. Each of the three HTR models (M1R1/R, M2R1/R, and P1R1/R) was implanted into the flanks of castrated male mice, all of which initially carried a testosterone pellet.

For these cohorts, 8 (4 with testosterone removed, 4 retained), 11 (4 removed, 7 retained), and 9 (3 removed, 6 retained) mice were included, respectively. Mice were paired by comparable tumor volumes, with one member undergoing pellet removal and the other retaining it. For animals surviving beyond 90 days, the testosterone pellet was replaced.

Figure 4 illustrates tumor volumes for each HTR model with and without testosterone. Despite intermodel variability, tumor regression after pellet removal was observed in at least some mice across all groups, with the P1R1/R line showing the strongest reduction following testosterone withdrawal.

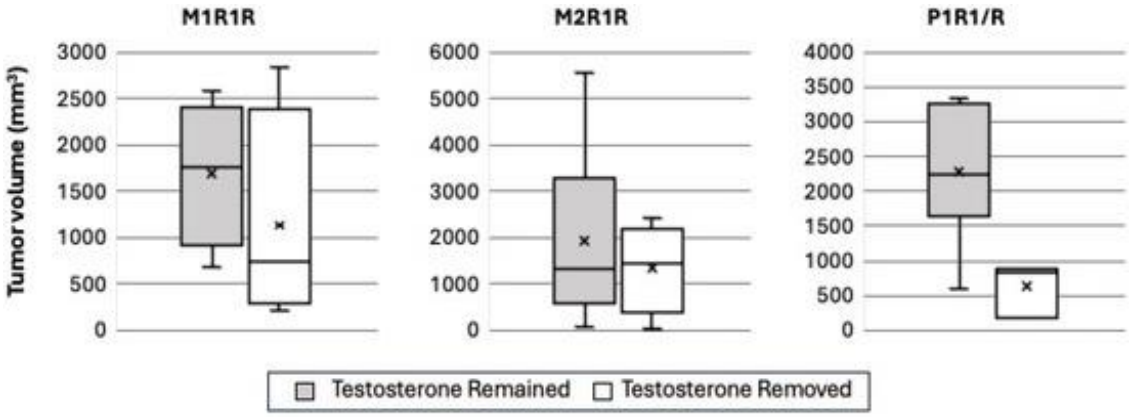

Figure 4. Tumor volume outcomes following testosterone pellet removal in HTR models.

Tumor volumes for mice retaining or losing testosterone pellets are presented at Day 30 or at euthanasia if performed earlier due to tumor burden. The central black line marks the median, the box encloses the 25th–75th percentiles, whiskers indicate the 5th–95th percentiles, and x represents the mean.

The overall survival curves for these HTR models are shown in **Figure 5**, revealing modest increases in survival after testosterone removal across all three lines. Nonetheless, given the limited sample sizes, none of these differences reached statistical significance.

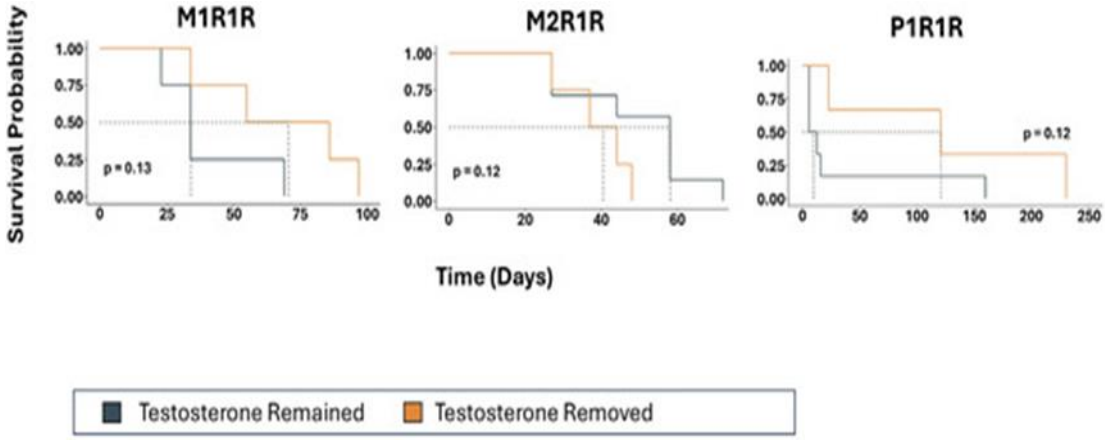

Figure 5. Overall survival in mice implanted with tumor cell variants exposed to high concentrations of testosterone (M1R1R, M2R1R, and P1R1R) in the presence of a testosterone pellet. Animals were subsequently assigned to either testosterone withdrawal (orange) or testosterone maintenance (black) groups. Day zero represents the initiation of testosterone removal or the corresponding control pairing where the testosterone pellet was retained.

Evaluation of androgen receptor (AR) expression

Androgen receptor (AR) signaling is thought to have a significant oncogenic influence on the emergence of castration resistance and on tumor sensitivity to supraphysiologic testosterone levels [18, 19]. We anticipated observable variations in AR expression among both castration-resistant and high-dose testosterone-resistant cell lines, as well as within individual model systems. AR expression was quantified by determining an H-score from randomly selected tumor slides obtained from animals bearing each cell line.

The mean (±SD) H-scores were 87.8 (22.5) for M1, 130.5 (27.2) for M2, and 218.8 (41.5) for P1. For their resistant counterparts—M1R1/R, M2R1/R, and P1R1/R—the mean (±SD) H-scores were 85.5 (17.9), 84.0 (14.8), and 122.8 (19.5), respectively. When comparing groups, the high-dose testosterone–sensitive CRPC lines averaged an H-score of 145 (62), whereas resistant CRPC lines averaged 97 (25). Once adjusted for repeated measures per

slide, this contrast did not reach statistical significance, likely reflecting variability within each cell line category. A correlation existed between AR expression level, its consistency (H-score), and response to testosterone treatment (P1 > M2 > M1, overall survival shown in **Figure 3**).

Among the HTR cell lines, AR intensity showed less fluctuation than in the CRPC lines. To further characterize AR expression diversity in tumors from both CRPC and HTR groups, the single-cell distribution of AR staining is displayed in **Figure 6**. Within the P1 CRPC model—the variant most responsive to high testosterone therapy—over 85% of cells were graded 2+ or 3+ for AR intensity, yielding the highest H-score (218.8). The M2 variant followed, with 39.3% of cells scored 2+ or 3+, and an intermediate H-score (130.5). The M1 model, least responsive to androgen therapy in vivo, contained only 0.3% of 3+ expressors, with more than 90% of cells showing either negative or faint staining (H-score 87.8).

In vitro induction of androgen resistance reduced AR expression levels in the P1 and M2 lineages but not in M1. Across hormonal conditions—whether androgen-depleted or androgen-saturated—subpopulations consistently persisted, containing both high AR expressors and AR-negative cells. This persistent heterogeneity likely underlies the tumor cells' adaptive capacity to survive under varying hormonal pressures.

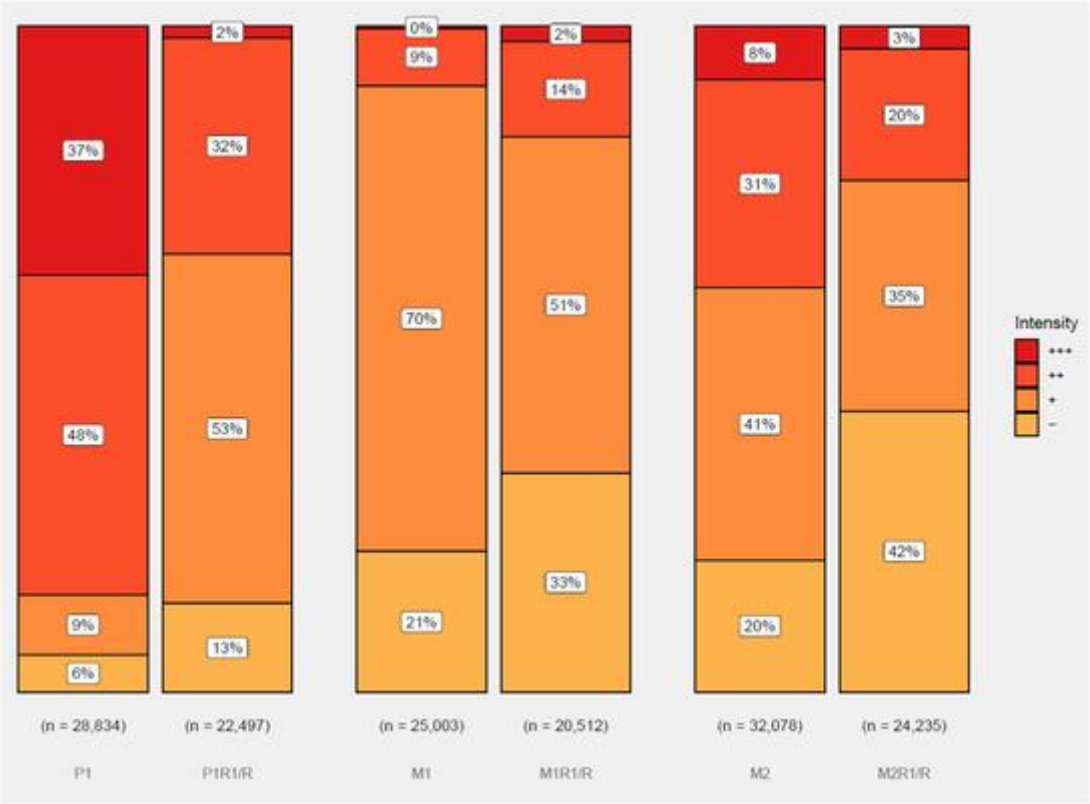

Figure 6. Androgen receptor (AR) expression in parental CRPC cell lines and their high-dose testosterone–resistant derivatives. Cells were classified based on AR staining intensity (0–3+), denoted as – for 0, + for 1+, ++ for 2+, and +++ for 3+. In each pair, the left column represents the parental lines (P1, M1, M2), and the right column represents their resistant derivatives (P1R1/R, M1R1/R, M2R1/R).

As supraphysiologic testosterone therapy becomes increasingly utilized in CRPC management, additional studies are essential to clarify the molecular drivers of resistance and to develop combination regimens. A key difficulty lies in replicating the variable clinical responses observed among patients with CRPC. Reported clinical response rates to high-dose testosterone range from 17% to 80%, with considerable variation in duration [13, 14, 20-23]. To address this variability, we generated three independently derived paired models—each consisting of a high-dose testosterone–sensitive and a high-dose testosterone–resistant CRPC line. Their distinct in vitro and in vivo reactions to testosterone treatment or withdrawal, together with differential AR staining profiles, closely parallel the heterogeneity noted in patients. These models therefore provide a valuable experimental platform for preclinical testing and therapeutic development in this underexplored disease subtype.

A frequent adaptive mechanism in prostate tumors under androgen-deprived conditions is an upregulation of AR protein expression [19, 24-26]. When these high-AR–expressing cells are subjected to supraphysiologic testosterone, AR binding sites become saturated, leading to nuclear accumulation and suppression of proliferation, often resulting in cell death [24]. This effect is most evident in the P1 model, which shows the highest AR expression (H-score 218.8) and demonstrates a testosterone-induced lifespan extension approaching one year.

The M2 line expresses intermediate AR levels—higher than M1, but lower than P1—and shows a corresponding survival outcome between the two. M1 has very few cells with strong (3+) AR expression, though roughly 80% exhibit some degree of AR positivity. Tumor volume reduction was apparent after 30 days of treatment, but this effect was not sustained, and overall survival improved only slightly.

These data reinforce that consistently elevated AR expression correlates with the strongest response to high-androgen therapy, while lower or more heterogeneous AR expression aligns with only temporary or minimal therapeutic benefit.

The generation of HTR variants from the three parent cell line models in culture produced cell lines capable of forming tumors efficiently in testosterone-supplemented, castrated, athymic mice. Tumors derived from these HTR lines displayed only a limited response following the removal of testosterone supplementation. Although some alteration in overall survival was observed across all three HTR variants, none of the small experimental cohorts demonstrated a statistically significant improvement. Early clinical observations in men who develop resistance to high-androgen therapy reveal that many still respond positively to subsequent treatment with the androgen receptor inhibitor enzalutamide [13]. This implies that resistance arising during high-androgen therapy may re-establish tumor sensitivity to hormonal interventions, though usually with diminished effectiveness. Resistance to androgen deprivation therapy, however, can emerge through multiple mechanisms beyond the androgen receptor pathway. Various forms of androgen-independent prostate cancer have been identified, most notably neuroendocrine (NE) prostate cancer, though other phenotypes lacking NE features but exhibiting minimal or absent AR-related gene expression have also been reported [27, 28]. Although previous studies have shown that culturing LNCaP cells in androgen-depleted media or in the presence of enzalutamide can induce neuroendocrine differentiation, no histologic evidence of such transformation was observed in our models [29, 30].

We confirmed that both gene-level and tumor-level differences exist among the individual cell lines in the HTR and testosterone-sensitive categories. Future investigations will focus on a more detailed examination of the genomic, transcriptomic, and metabolomic profiles of these models. Such insights will enable the development and testing of new therapeutic approaches for high-dose testosterone resistance, an emerging clinical condition, as the use of high-dose testosterone in CRPC treatment continues to expand. Several recent and ongoing clinical trials are already evaluating this approach (e.g., NCT04704505, NCT05011383, NCT04363164, NCT03734653).

Conclusion

In conclusion, we have established multiple preclinical models of both CRPC and high-dose testosterone–resistant prostate cancer that accurately reproduce the clinical heterogeneity observed in patients. These models provide a valuable system for exploring the molecular mechanisms underlying high-dose testosterone resistance and for developing potential new therapeutic strategies. Ongoing studies aim to further define the molecular determinants driving resistance in these HTR models, alongside concurrent drug development efforts to identify promising candidates for future clinical evaluation.

Acknowledgments: None

Conflict of Interest: None

Financial Support: None

Ethics Statement: None

References

1. American Cancer Society. Cancer Facts & Figures 2022. Atlanta (GA): American Cancer Society; 2022.

2. Siegel RL, Giaquinto AN, Jemal A. Cancer statistics, 2024. CA Cancer J Clin. 2024;74(1):12–49.
3. Hussain M, Fizazi K, Shore ND, Heidegger I, Smith MR, Tombal B, et al. Metastatic hormone-sensitive prostate cancer and combination treatment outcomes: A review. JAMA Oncol. 2024;10(6):807–20.
4. Fizazi K, Scher HI, Molina A, Logothetis CJ, Chi KN, Jones RJ, et al. Abiraterone acetate for treatment of metastatic castration-resistant prostate cancer: Final overall survival analysis of the COU-AA-301 randomised, double-blind, placebo-controlled phase 3 study. Lancet Oncol. 2012;13(10):983–92.
5. Scher HI, Fizazi K, Saad F, Taplin ME, Sternberg CN, Miller K, et al. Increased survival with enzalutamide in prostate cancer after chemotherapy. N Engl J Med. 2012;367(13):1187–97.
6. Fizazi K, Shore N, Tammela TL, Ulys A, Vjaters E, Polyakov S, et al. Darolutamide in nonmetastatic, castration-resistant prostate cancer. N Engl J Med. 2019;380(13):1235–44.
7. Kantoff PW, Higano CS, Shore ND, Berger ER, Small EJ, Penson DF, et al. Sipuleucel-T immunotherapy for castration-resistant prostate cancer. N Engl J Med. 2010;363(5):411–22.
8. Parker C, Nilsson S, Heinrich D, Helle SI, O'Sullivan JM, Fossa SD, et al. Alpha emitter radium-223 and survival in metastatic prostate cancer. N Engl J Med. 2013;369(3):213–23.
9. Kellokumpu-Lehtinen PL, Harmenberg U, Joensuu T, McDermott R, Hervonen P, Ginman C, et al. 2-Weekly versus 3-weekly docetaxel to treat castration-resistant advanced prostate cancer: A randomised, phase 3 trial. Lancet Oncol. 2013;14(2):117–24.
10. de Bono JS, Oudard S, Ozguroglu M, Hansen S, Machiels JP, Kocak I, et al. Prednisone plus cabazitaxel or mitoxantrone for metastatic castration-resistant prostate cancer progressing after docetaxel treatment: A randomised open-label trial. Lancet. 2010;376(9747):1147–54.
11. Sartor O, de Bono J, Chi KN, Fizazi K, Herrmann K, Rahbar K, et al. Lutetium-177–PSMA-617 for metastatic castration-resistant prostate cancer. N Engl J Med. 2021;385(12):1091–103.
12. Denmeade SR, Isaacs JT. Bipolar androgen therapy: The rationale for rapid cycling of supraphysiologic androgen/ablation in men with castration-resistant prostate cancer. Prostate. 2010;70(13):1600–7.
13. Denmeade SR, Wang H, Agarwal N, Smith DC, Schweizer MT, Stein MN, et al. TRANSFORMER: A randomized phase II study comparing bipolar androgen therapy versus enzalutamide in asymptomatic men with castration-resistant metastatic prostate cancer. J Clin Oncol. 2021;39(12):1371–82.
14. Teply BA, Wang H, Luber B, Sullivan R, Rifkind I, Bruns A, et al. Bipolar androgen therapy in men with metastatic castration-resistant prostate cancer after progression on enzalutamide: An open-label, phase 2, multicohort study. Lancet Oncol. 2018;19(1):76–86.
15. Nordeen SK, Su LJ, Osborne GA, Hayman PM, Orlicky DJ, Wessells VM, et al. Titration of androgen signaling: How basic studies have informed clinical trials using high-dose testosterone therapy in castrate-resistant prostate cancer. Life. 2021;11(9):884.
16. Sedelaar JP, Dalrymple SS, Isaacs JT. Of mice and men—Warning: Intact versus castrated adult male mice as xenograft hosts are equivalent to hypogonadal versus abiraterone treated aging human males, respectively. Prostate. 2013;73(12):1316–25.
17. Qiu PH, Sheng J. A two-stage procedure for comparing hazard rate functions. J R Stat Soc B. 2008;70(1):191–208.
18. Mohammad OS, Nyquist MD, Schweizer MT, Balk SP, Corey E, Plymate S, et al. Supraphysiologic testosterone therapy in the treatment of prostate cancer: Models, mechanisms and questions. Cancers. 2017;9(12):166.
19. Chen CD, Welsbie DS, Tran C, Baek SH, Chen R, Vessella R, et al. Molecular determinants of resistance to antiandrogen therapy. Nat Med. 2004;10(1):33–9.
20. Markowski MC, Taplin ME, Aggarwal R, Sena LA, Wang H, Qi H, et al. Bipolar androgen therapy plus nivolumab for patients with metastatic castration-resistant prostate cancer: The COMBAT phase II trial. Nat Commun. 2024;15(1):14.
21. Markowski MC, Wang H, Sullivan R, Rifkind I, Sinibaldi V, Schweizer MT, et al. A multicohort open-label phase II trial of bipolar androgen therapy in men with metastatic castration-resistant prostate cancer (RESTORE): A comparison of post-abiraterone versus post-enzalutamide cohorts. Eur Urol. 2021;79(5):692–9.
22. Schweizer MT, Antonarakis ES, Wang H, Ajiboye AS, Spitz A, Cao H, et al. Effect of bipolar androgen therapy for asymptomatic men with castration-resistant prostate cancer: Results from a pilot clinical study. Sci Transl Med. 2015;7(269):269ra262.

23. Schweizer MT, Wang H, Luber B, Nadal R, Spitz A, Rosen DM, et al. Bipolar androgen therapy for men with androgen ablation-naïve prostate cancer: Results from the phase II BATMAN study. Prostate. 2016;76(13):1218–26.
24. Isaacs JT, D'Antonio JM, Chen S, Antony L, Dalrymple SP, Ndikuyeze GH, et al. Adaptive auto-regulation of androgen receptor provides a paradigm shifting rationale for bipolar androgen therapy (BAT) for castrate-resistant human prostate cancer. Prostate. 2012;72(14):1491–505.
25. Aurilio G, Cimadamore A, Mazzucchelli R, Lopez-Beltran A, Verri E, Scarpelli M, et al. Androgen receptor signaling pathway in prostate cancer: From genetics to clinical applications. Cells. 2020;9(10):2653.
26. Graham L, Schweizer MT. Targeting persistent androgen receptor signaling in castration-resistant prostate cancer. Med Oncol. 2016;33(4):44.
27. Bluemn EG, Coleman IM, Lucas JM, Coleman RT, Hernandez-Lopez S, Tharakan R, et al. Androgen receptor pathway-independent prostate cancer is sustained through FGF signaling. Cancer Cell. 2017;32(3):474–89.e6.
28. Labrecque MP, Coleman IM, Brown LG, True LD, Kollath L, Lakely B, et al. Molecular profiling stratifies diverse phenotypes of treatment-refractory metastatic castration-resistant prostate cancer. J Clin Invest. 2019;129(10):4492–505.
29. Farach A, Ding Y, Lee M, Creighton C, Delk NA, Ittmann M, et al. Neuronal trans-differentiation in prostate cancer cells. Prostate. 2016;76(12):1312–25.
30. Shen R, Dorai T, Szaboles M, Katz AE, Olsson CA, Buttyan R. Transdifferentiation of cultured human prostate cancer cells to a neuroendocrine cell phenotype in a hormone-depleted medium. Urol Oncol. 1997;3(2):67–75.